CHAPTER 3: RESULTS

3.1 Influent characteristics

Average influent temperature at STP 1, 2 and 3 were 28.8 ± 0.5, 29.2 ± 1.3 and 30.6 ± 0.8°C, respectively, whereas average influent pH in STP 1, 2 and 3 were 7.0 ± 0.6, 6.8 ± 0.8 and 6.2 ± 0.8, respectively.

From Figure 3.1, average influent DO was the highest at STP 1 (4.0 ± 1.8 mg l^{-1}), followed by STP 2 (2.6 ± 1.4 mg l^{-1}) and STP 3 (1.3 ± 1.1 mg l^{-1}). Influent BOD and COD were not significantly different at all STPs, and ranged from 140 to 480 mg l^{-1} and 320 to 1240 mg l^{-1}, respectively.

Nutrient concentrations in the influent are shown in Table 3.1. Both influent ammonia and phosphate concentrations were high at STP 1, 2 and 3 and averaged from 44.40 ± 4.80 mg l^{-1} to 50.10 ± 2.30 mg l^{-1} and 50.30 ± 11.80 mg l^{-1} to 62.80 ± 12.40 mg l^{-1}, respectively. Nitrite concentrations in influent at the three STPs were below 0.35 mg l^{-1} whereas nitrate concentrations in STP 1, 2 and 3 were 0.83 ± 0.47 mg l^{-1}, 2.52 ± 3.79 mg l^{-1} and 2.04 ± 3.46 mg l^{-1}, respectively.

Heavy metal concentration in the influent of each STP is shown in Table 3.2. As concentrations in the influent of STP 1, 2 and 3 were generally low and averaged 0.001 ± 0 mg l^{-1}, 0.006 ± 0.004 mg l^{-1} and 0.001 ± 0 mg l^{-1}, respectively. Similarly, Cd and Hg concentrations were below 0.002 mg l^{-1} and 0.001 mg l^{-1}, respectively. Cr concentration in the influent of all STPs ranged from 0.002 ± 0 mg l^{-1} to 0.011 ± 0.016 mg l^{-1}. By contrast, Cu and Pb concentrations were significantly higher at STP 3 (0.305 ± 0.450 mg l^{-1} and 0.625 ± 0.084 mg l^{-1}, respectively) than STP 1 ($q > 9.36$, $p < 0.01$) and STP 2 ($q > 9.20$, $p < 0.01$).

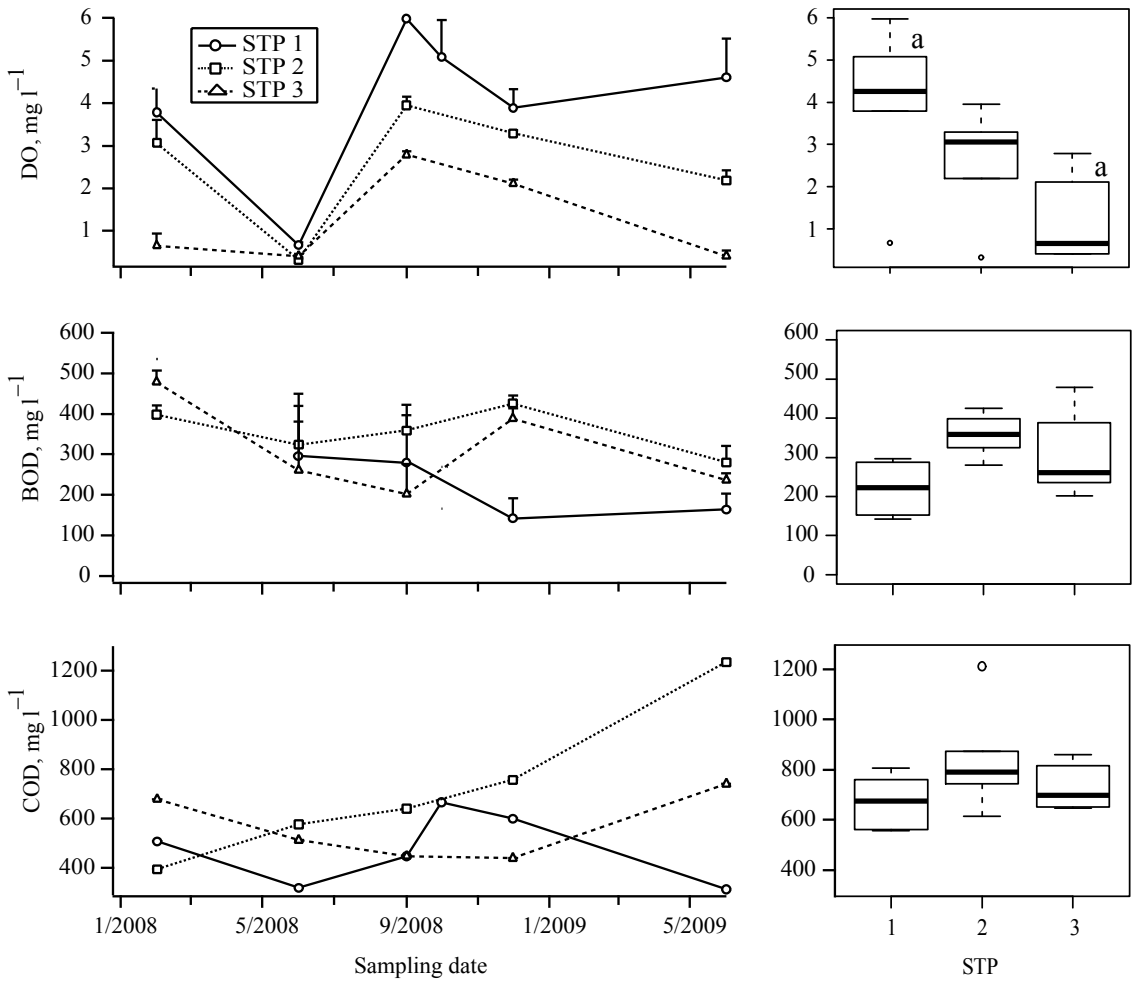

Figure 3.1: Left panel shows the DO, BOD_5 and COD concentrations in the influent at each STP throughout the sampling period. Right panel shows the respective box plot indicating median, and range of the profiles. Outliers are also shown as open circles. The same letters of the alphabet are used to indicate values whose means were significantly different.

Table 3.1: Nutrient concentration (mg l^{-1}) in each STP.

Nutrients	STP 1 (n = 6)	STP 2 (n = 5)	STP 3 (n = 5)
Influent			
NH_3	44.40 ± 4.80	50.10 ± 2.30	44.70 ± 6.10
NO_2^-	0.20 ± 0.07	0.35 ± 0.06	0.32 ± 0.25
NO_3^-	0.83 ± 0.47	2.52 ± 3.79	2.04 ± 3.46
PO_4^{3-}	50.30 ± 11.80	62.80 ± 12.40	52.70 ± 45.70
Aerationtank			
NH_3	0.90 ± 0.70	21.70 ± 10.10	8.30 ± 13.90
NO_2^-	0.27 ± 0.09	0.27 ± 0.20	0.48 ± 0.33
NO_3^-	14.02 ± 18.36	30.02 ± 26.04	45.79 ± 24.70
PO_4^{3-}	50.00 ± 20.00	43.00 ± 33.80	10.55 ± 6.09
Effluent			
NH_3	3.00 ± 6.40	37.50 ± 9.90	2.60 ± 1.00
NO_2^-	0.20 ± 0.20	2.13 ± 2.15	0.68 ± 0.44
NO_3^-	25.80 ± 24.90	28.41 ± 25.02	36.12 ± 22.88
PO_4^{3-}	40.90 ± 14.10	84.90 ± 16.20	9.50 ± 4.80

For complete data, please refer to Appendix F, G and H.

Table 3.2: Heavy metal concentration (mg l^{-1}) at each STP (n = 3).

Heavy metal	STP 1	STP 2	STP 3
Influent			
As	0.001 ± 0.000	0.006 ± 0.004	0.001 ± 0.000
Cd	0.001 ± 0.000	0.002 ± 0.000	0.001 ± 0.000
Cr	0.002 ± 0.000	0.004 ± 0.005	0.011 ± 0.016
Cu	0.006 ± 0.005	0.007 ± 0.005	<u>0.305 ± 0.450</u>
Pb	0.020 ± 0.022	0.010 ± 0.000	<u>0.625 ± 0.084</u>
Hg	0.001 ± 0.000	0.001 ± 0.000	0.001 ± 0.000
Aeration tank			
As	0.012 ± 0.009	0.002 ± 0.002	0.016 ± 0.007
Cd	0.002 ± 0.000	0.002 ± 0.000	0.024 ± 0.019
Cr	0.021 ± 0.010	0.009 ± 0.002	0.327 ± 0.337
Cu	0.187 ± 0.181	0.055 ± 0.027	6.065 ± 3.062
Pb	0.029 ± 0.030	0.020 ± 0.017	4.250 ± 2.580
Hg	0.001 ± 0.000	0.001 ± 0.000	0.001 ± 0.001

Underlined figures are statistically significant using ANOVA and Tukey test.

3.2 Physico-chemical characteristics in the aeration tank

Average temperature in the aeration tank of STP 1, 2 and 3 were 27.5 ± 0.4, 29.7 ± 0.6 and 31.3 ± 1.2°C, respectively whereas average pH in STP 1, 2 and 3 were 6.0 ± 0.9, 6.0 ± 0.7 and 5.0 ± 0.7, respectively. Ammonium in the aeration tanks of STP 1, 2 and 3 reduced to 0.90 ± 0.70 mg l^{-1}, 21.70 ± 10.10 mg l^{-1} and 8.30 ± 13.90 mg l^{-1}, respectively whereas nitrate increased to 14.02 ± 18.36 mg l^{-1}, 30.02 ± 26.04 mg l^{-1} and 45.79 ± 24.70 mg l^{-1}, respectively (Table 3.1). Nitrite in the aeration tanks of all the STPs were below 0.48 ± 0.33 mg l^{-1}, and phosphate in STP 1, 2 and 3 were 50.00 ± 20.00 mg l^{-1}, 43.00 ± 33.80 mg l^{-1} and 10.55 ± 6.09 mg l^{-1}, respectively.

Cu in the aeration tank of STP 3 (6.065 ± 3.062 mg l^{-1}) was higher than STP 1 ($q = 6.86$, $p < 0.05$) and STP 2 ($q = 7.01$, $p < 0.01$) (F = 14.04, $df = 7$, $p < 0.001$) (Table 3.2). Similarly, Pb at STP 3 (4.250 ± 2.580 mg l^{-1}) was also higher than STP 1 ($q = 4.91$, $p < 0.05$) and STP 2 ($q = 4.92$, $p < 0.05$) (F = 8.04, $df = 8$, $p < 0.05$).

SV was significantly different among the three STPs (F = 30.52, $df = 13$, $p < 0.001$) (Figure 3.2). SV at STP 1 ranged from 440 to 980 mg l^{-1}, and was the highest compared with STP 2 ($q = 8.25$, $p < 0.001$) and STP 3 ($q = 9.54$, $p < 0.001$). MLSS at STP 1 (F = 22.88, $df = 13$, $p < 0.001$) ranged from 3832 to 6340 mg l^{-1}, and was also the highest compared with STP 2 ($q = 4.62$, $p < 0.05$) and STP 3 ($q = 9.21$, $p < 0.001$). STP 2 also showed higher MLSS relative to STP 3 ($q = 4.59$, $p < 0.05$). Similarly, MLVSS at STP 1 (F = 60.59, $df = 13$, $p < 0.001$) was higher than STP 2 ($q = 7.60$, $p < 0.0.001$) and STP 3 ($q = 14.96$, $p < 0.001$). MLVSS at STP 2 was also higher than STP 3 ($q = 7.36$, $p < 0.001$).

Flocs in STP 1 were well developed with an average size of 0.246 ± 0.227 mm^2, followed by STP 2 (0.128 ± 0.079 mm^2) whereas STP 3 had pin point flocs with an average size of 0.083 ± 0.077 mm^2.

DOUR in the aeration tanks was significantly different among the three STPs ($F = 6.69$, $df = 15$, $p < 0.05$). STP 3 had an average DOUR of 663 ± 208 mg l^{-1} hr^{-1}, which was significantly lower than STP 1 (907 ± 101 mg l^{-1} hr^{-1}, $q = 4.66$, $p < 0.05$) and STP 2 (888 ± 213 mg l^{-1} hr^{-1}, $q = 4.38$, $p < 0.05$).

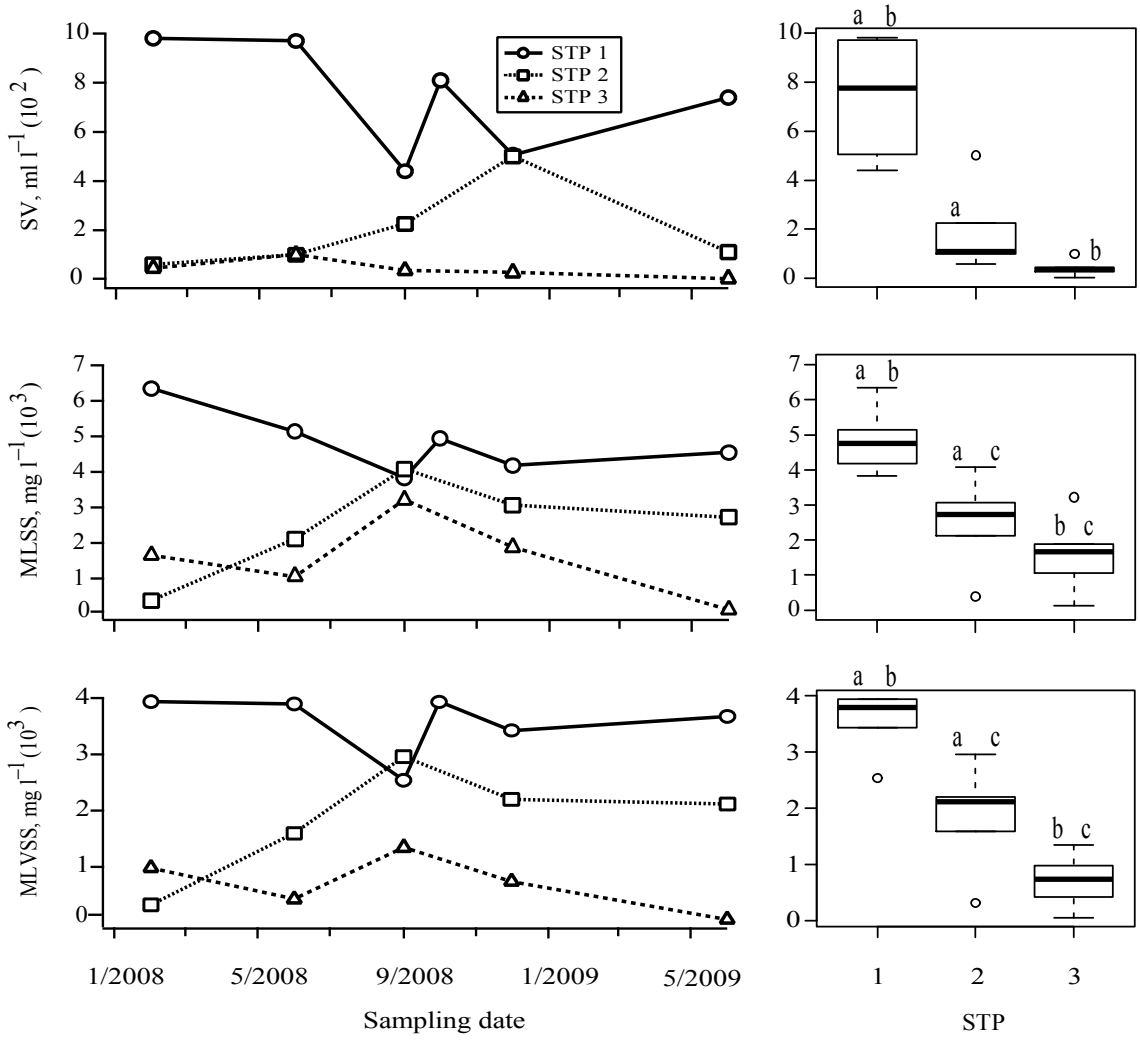

Figure 3.2: Left panel shows the SV, MLSS and MLVSS measured from aeration tank at each STP throughout the sampling period. Right panel shows the respective box plot indicating median, and range of the profiles. Outliers are also shown as open circles. The same letters of the alphabet are used to indicate values whose means were significantly different.

3.3 Effluent characteristics

Effluent TSS (Figure 3.3) from all STPs ranged from 9 to 163 mg l^{-1}. STP 3 had the highest TSS in the effluent with an average of 76.60 ± 53.89 mg l^{-1} whereas STP 1 was below 50 mg l^{-1} throughout all the samplings.

Similarly, both reduction efficiency of BOD and COD were poor in STP 3 at 38% and 49%, respectively whereas STP 1 showed highest BOD and COD reduction efficiency of 76% and 61%, respectively. The BOD and COD reduction efficiency in STP 2 were 40% and 42%, respectively.

Effluent DO ranged from 0.93 ± 0.10 mg l^{-1} to 5.29 ± 0.44 mg l^{-1}.

Ammonia in the effluent of all the STPs ranged from 0.45 ± 0.33 mg l^{-1} to 41.75 ± 1.83 mg l^{-1} whereas nitrite in the effluent of all the STPs were below 2.13 mg l^{-1}. The average nitrate concentration for all the STPs ranged from 25.81 ± 1.50 mg l^{-1} to 36.12 ± 1.92 mg l^{-1}. Effluent phosphate ranged from 9.46 ± 4.88 mg l^{-1} to 85.86 ± 60.26 mg l^{-1}.

Table 3.3: Removal efficiency of BOD and COD at STP 1, 2 and 3.

	BOD		COD	
	Average (mg l^{-1})	Removal efficiency (%)	Average (mg l^{-1})	Removal efficiency (%)
STP 1 Influent	220 ± 79		476 ± 0.2	
STP 1 Effluent	34 ± 24	83	113 ± 0.2	73
STP 2 Influent	357 ± 54		523 ± 0.2	
STP 2 Effluent	222 ± 87	40	393 ± 0.2	42
STP 3 Influent	312 ± 53		567 ± 0.1	
STP 3 Effluent	184 ± 62	39	253 ± 0.1	53

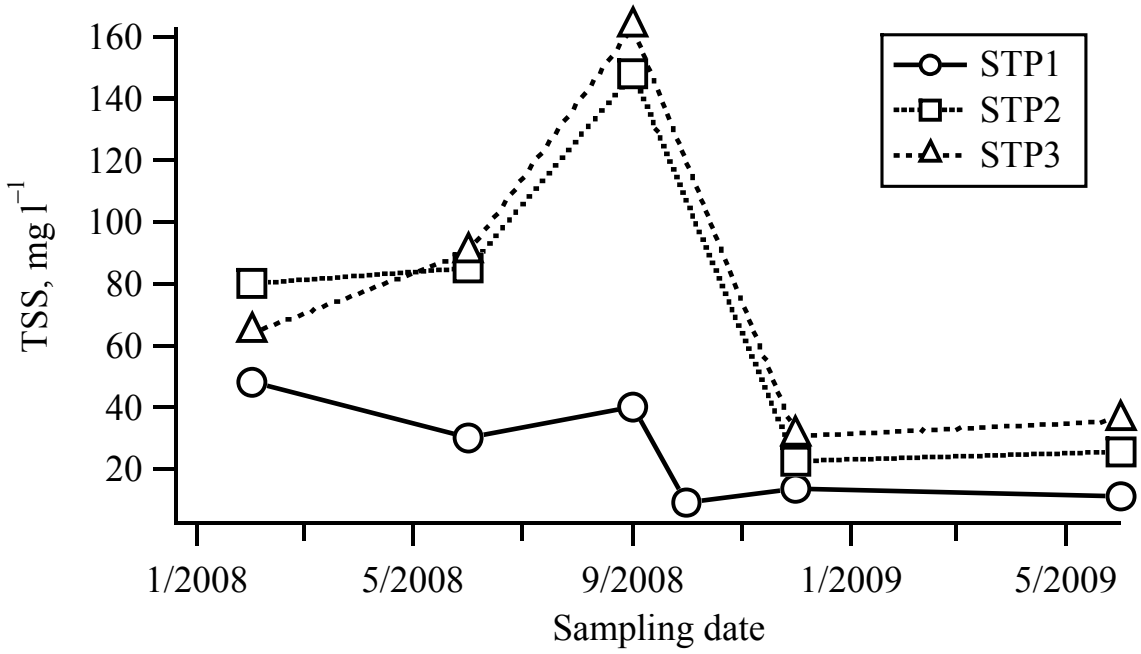

Figure 3.3: TSS (mg l^{-1}) of the effluent in each STP throughout the sampling period.

3.4 Bacterial profiling

Total DNA from activated sludge samples of each sampling was extracted using a modified chemical-enzymatic lysis method. A total of 16 extracted DNA were examined with gel electrophoresis (Figure 3.4).

From the extracted genomic material of the activated sludge, partial 16S rRNA gene of about 600bp was amplified (Figure 3.5).

DGGE analysis of 16S rRNA fragment (Figure 3.6) was then carried out to investigate bacterial community profiles in activated sludge systems from all the STPs. DGGE was used to resolve the partial 16S rRNA PCR amplicons. The number of bands per lane varied from 13 to 22. Selected bands were extracted and sequenced (Table 3.4) for identifications coverage at each site averaged from 84 to 89%. DGGE profiles at STP 1 showed a total of 37 unique OTUs detected compared to 40 OTUs at STP 2 and 35 OTUs at STP 3.

Cluster analysis of the DGGE profiles showed that the microbial populations were extended over 6 samplings from the same STPs tend to group together at a similarity > 0.5 (Figure 3.7).

Maximum likelihood trees showed that the total bacterial community from STP 1, 2 and 3 composed of eight groups of bacteria i.e. *α-Proteobacteria, β-Proteobacteria, γ-Proteobacteria, δ-Proteobacteria*, *Bacteroidetes*, *Acidobacteria*, *Nitrospirae* and *Chloroflexi* (Figures 3.8, 3.9 and 3.10). At STP 1, all eight groups were detected whereas for STP 2 and 3, only seven groups were detected. *Chloroflexi* was detected only in STP 1. All the three STPs were dominated by *β-Proteobacteria* with 43% (n = 16) in STP 1, 38% (n = 15) in STP 2 and 44% (n = 16) in STP 3. This was followed by *Bacteroidetes* where 16% (n = 6) were found in STP 1, 25% (n = 10) in STP 2 and 19% (n = 7) in STP 3.

From the presence-absence matrix (Appendix I), we used analysis of similarity (ANOSIM) and showed that STP 1 was significantly different from both STP 2 ($p = 0.002$) and STP 3 ($p = 0.003$). Similarity percentage (SIMPER) test showed that for the difference between STP 1 and STP 3, OTU 14, OTU 42 and OTU 28 were the most important. OTU 14 and OTU 42 i.e. uncultured *Flavobacterium* sp. and uncultured *Acidobacteriales* were more prevalent at STP 3, whereas OTU 28 (uncultured *Thiobacillus* sp.) was more prevalent at STP 1. Between STP 1 and STP 2, the most important OTUs were OTU 14, OTU 12 and OTU 29. OTU 14 and OTU 12 were more prevalent at STP 2, whereas OTU 29 was more prevalent at STP 1. OTU 12 was the uncultured *Saprospiraceae* sp., whereas OTU 29 was the uncultured *Sterolibacterium* sp.

Ecological distance of the bacterial community structure was analyzed by the ordination technique of CCA. The selected environmental variables were SSV, DOUR, Cu and Pb. The CCA accounted for 81.5% variance whereas the first axis (CCA1) explained 48.1% variance (Figure 3.11). The observed relationship between environmental variables and ecological distance was not due to chance ($p < 0.05$), and we observed two distinct groups of bacteria that were placed away from the center. One group consisted of OTU 8, OTU 15 and OTU 16 which were uncultured *Sphingobacteriales* (OTU 8) and uncultured *Thermomonas* sp. (OTU 16). OTU 15 was not identified. Another group of bacteria consisted of OTU 30 (uncultured *Chloroflexi*), OTU 29 (uncultured *Sterolibacterium* sp.), OTU 22 (uncultured *Bradyrhizobium* sp.) and OTU 9 was not identified.

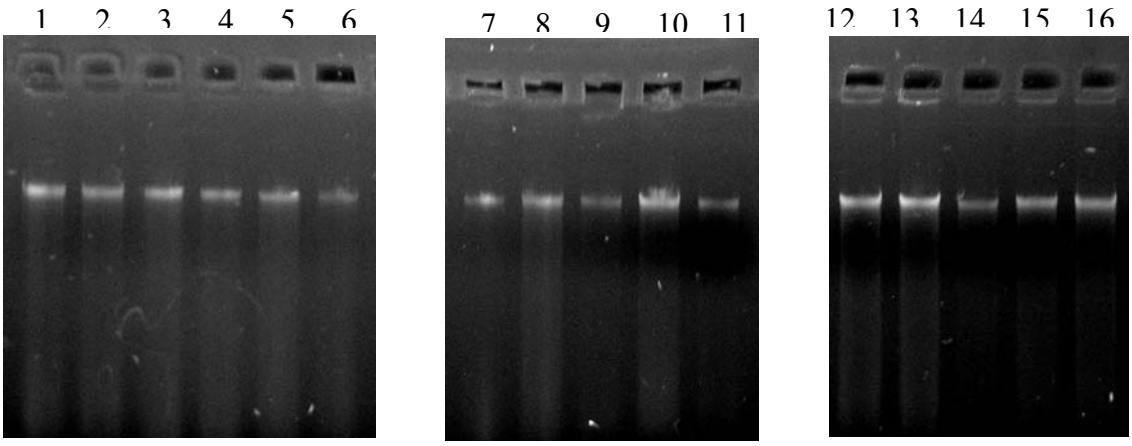

Figure 3.4: Agarose gel electrophoresis of extracted DNA (1 µl). Lane 1 to 6 are 6 different samplings for STP 1, lane 7 to 11 are 5 different samplings for STP 2 and lane 12 to 16 are for STP 3.

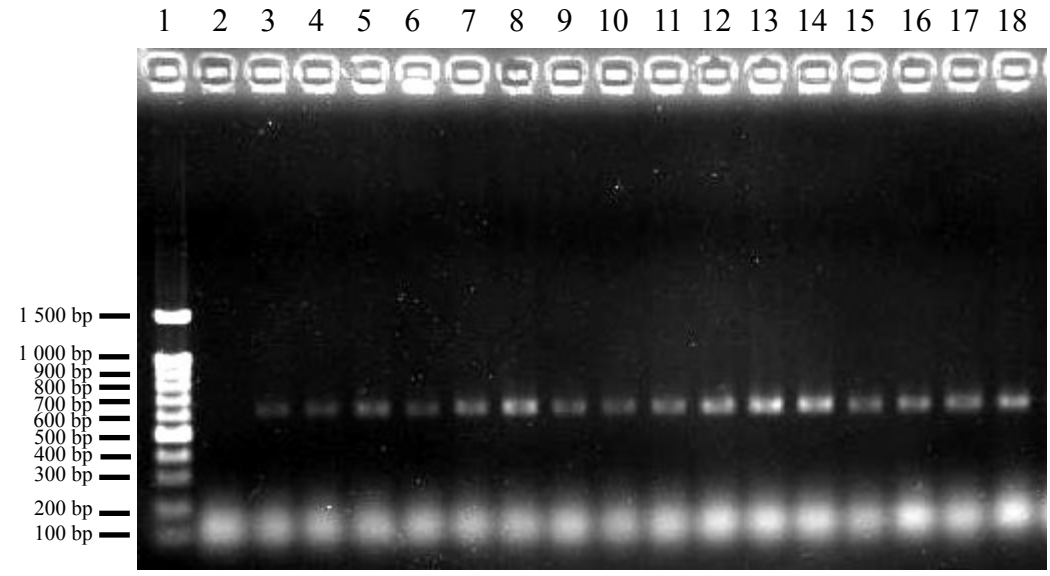

Figure 3.5: Agarose gel electrophoresis of amplified 16S rRNA. Lane 1 is 100 bp DNA ladder (iNtRON Biotechnology, Korea), lane 2 to 7 are from 6 samplings in STP 1, lane 8 to 12 are from 5 samplings in STP 2 and lane 13 to 18 are for STP 3.

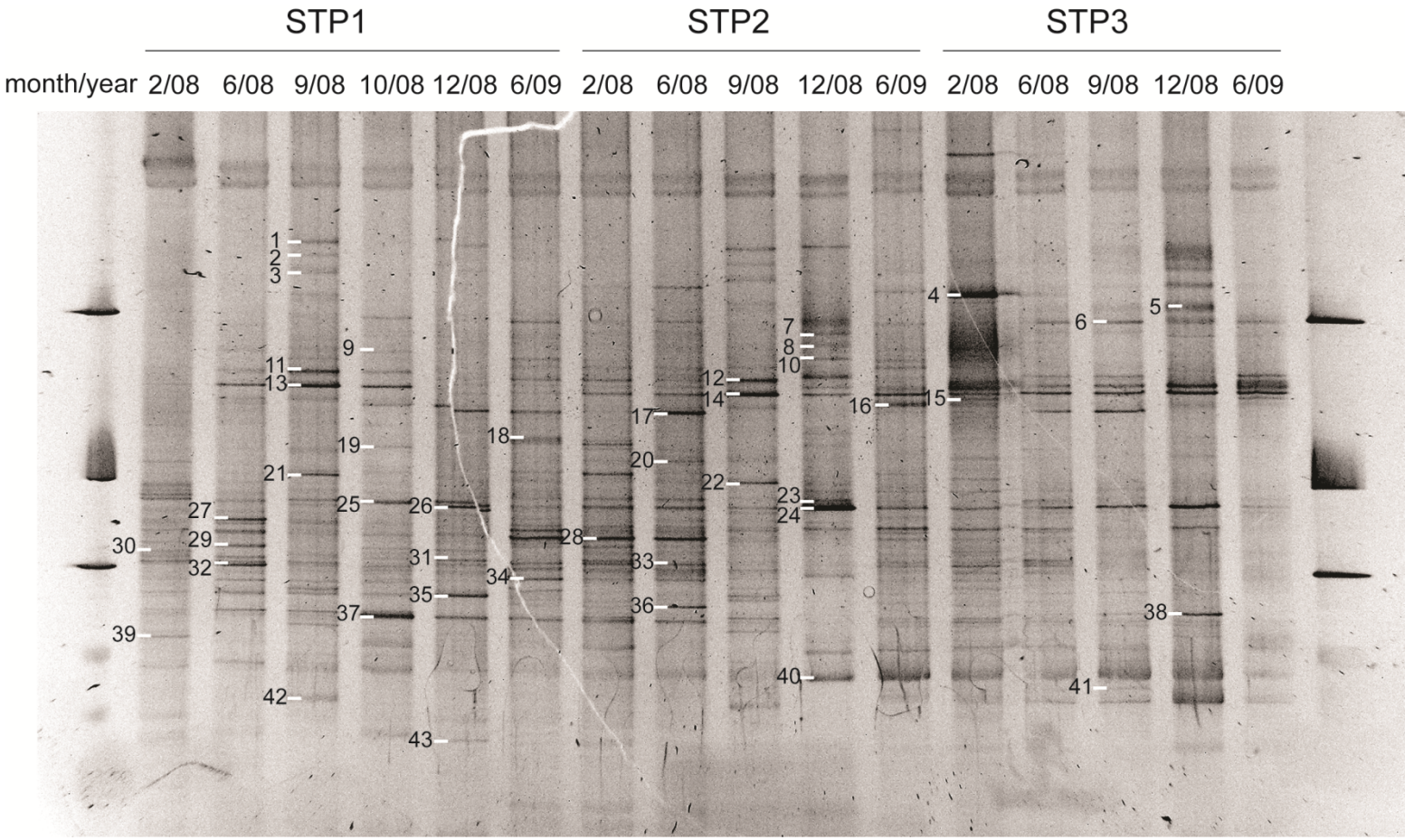

Figure 3.6: DGGE banding patterns of 16S rDNA fragments amplified using bacteria specific primers 314F-GC and 907R. Highlighted bands (with their OTU designation) were excised, reamplified and sequenced for phylogenetic analysis. The first and last lanes are in-house markers whereas Lanes 2 to 7 are the six different samplings for STP 1. Lanes 8 to 12 are for STP 2 whereas lanes 13 to 17 are for STP 3. The label indicates the month and year of sampling.

Table 3.4: Identity of extracted bands from DGGE gel in Figure 3.6.

Clone	Accession code	Homolog	Homolog accession	Similarity (%)
3	JF261089	Uncultured *Rhodocyclaceae* bacterium	GU257835	99
4	JF261090	Uncultured *Chloroflexi* bacterium	AM159381	99
7	JF423919	Uncultured Flavobacteria bacterium	EF665452	95
8	JF261091	Uncultured *Acidobacterium* sp.	EF125937	100
9	JF261092	Uncultured *Thiobacillus* sp.	DQ232862	99
10	JF261093	Uncultured *Sterolibacterium* sp.	EU283472	100
11	JF423920	Uncultured *Clostridium* sp.	GQ183377	99
12	JF423921	Uncultured Sphingobacteriales bacterium	EU298000	97
13	JF423922	Uncultured *Aquabacterium* sp.	EU043570	99
14	JF423923	Uncultured *Nitrospira* sp.	AJ224042	99
16	JF423924	Uncultured Sphingobacteriales bacterium	FJ536888	99
17	JF423925	Uncultured *Flavisolibacter* sp.	GQ287421	99
18	JF423926	Uncultured *Bacteroides* sp.	GU271248	99
19	JF423927	Uncultured *Roseobacter* sp.	AY569301	99
20	JF423928	Uncultured Acidobacteriales bacterium	EF073335	98
24	JF433957	Uncultured *Alicycliphilus* sp.	GU056299	99
25	JF433958	Uncultured *Nitrospira* sp.	HQ424561	99
26	JF433959	Uncultured *Rhodocyclaceae* bacterium	HM631993	97
27	JF433960	Uncultured *Thiobacillus thioparus*	HM173634	98
28	JF433961	Uncultured Acidobacteria bacterium	EF075172	100
29	JF433962	Uncultured *Nitrospira* sp.	DQ414435	99
33	JF433963	Uncultured *Hydrogenophaga* sp.	EU305579	99
34	JF433964	Uncultured *Saprospiraceae* bacterium	EU177764	100
35	JF433965	Uncultured *Flavobacterium* sp.	AJ871245	98
38	JF433966	Uncultured *Azonexus* sp.	GU056304	100
39	JF433967	Uncultured *Aquabacterium* sp.	GU319965	99
40	JF433968	Uncultured *Dechloromonas* sp.	GU202936	99
41	JF433969	Uncultured *Dechloromonas* sp.	AY126452	99
42	JF433970	Uncultured *Rhodocyclaceae* bacterium	HQ184350	99
43	JF433971	Uncultured *Pelobacter* sp.	DQ647155	97
44	JF699653	Uncultured *Pelobacter* sp.	EU328012	95
45	JF699654	Uncultured *Bacteroides* sp.	GU271459	98
47	JF699655	Uncultured *Rhodocyclaceae* bacterium	AM268359	99
48	JF699656	Uncultured *Bradyrhizobium* sp.	AB512186	98
49	JF699657	Uncultured Sphingobacteriales	HM346260	97
50	JF699658	Uncultured Sphingobacteriales bacterium	FJ037322	98

Table 3.4, continued

Clone	Accession code	Homolog	Homolog accession	Similarity (%)
51	JF699660	Uncultured *Ottowia* sp.	EU882843	97
50a	JF699659	Uncultured *Xanthomonadaceae* bacterium	EU299645	97
52	JF699661	Uncultured *Thermomonas brevis*	AB355702	98
53	JF699662	Uncultured *Flavisolibacter* sp.	GQ287421	99
54	JF699663	Uncultured *Thermomonas* sp.	EF633616	99
55	JF699664	Uncultured *Haliscomenobacter* sp.	AB543040	98
56	JF699665	Uncultured *Hydrogenophaga pseudoflava*	FJ947058	98
57	JF699666	Uncultured Gammaproteobacteria	GQ249377	99
59	JF699667	Uncultured *Comamonas aquatica*	FJ404812	99
60	JF699668	Uncultured Gammaproteobacteria bacterium	CU926678	99
63	JF699669	Uncultured *Hydrogenophaga* sp.	EU652485	99
69	JF699670	Uncultured *Lewinella* sp.	AB543041	99
76	JF699671	Uncultured *Luteimonas* sp.	EF648150	98

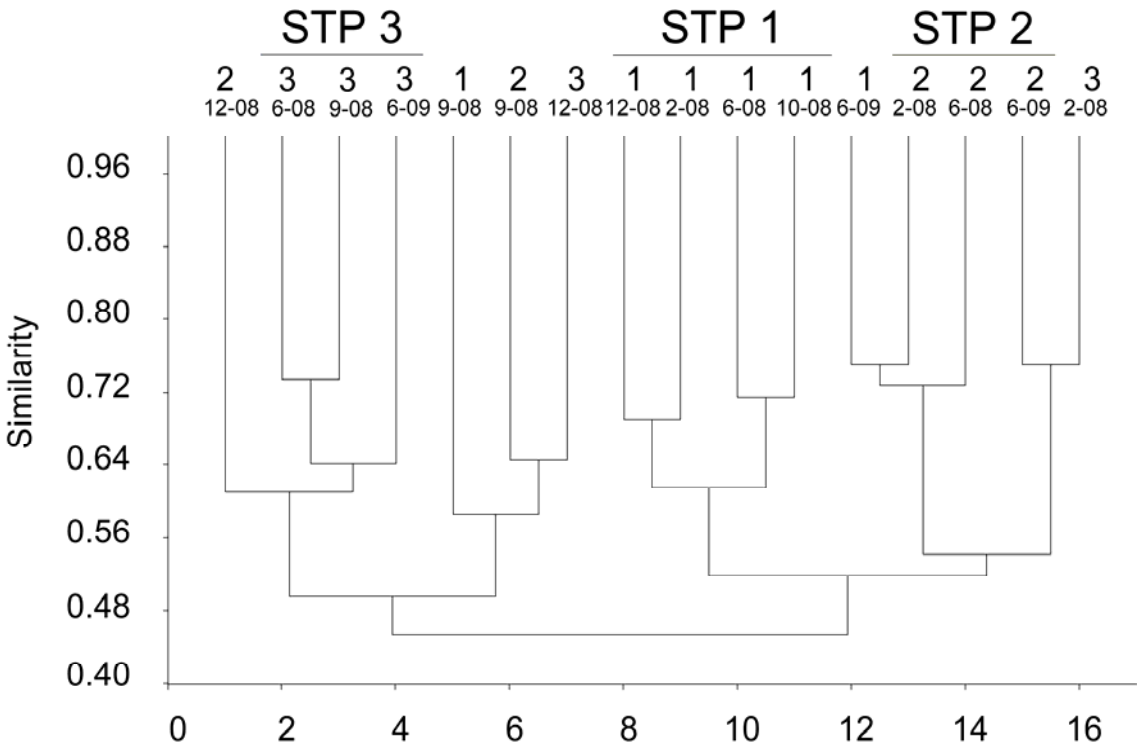

Figure 3.7: Dendrogram of similarity values between STPs on each sampling. The cluster analysis was based on the similarity matrix calculated using the Morishita coefficient. Each sampling was labeled according to the STP, and the month and year of sampling.

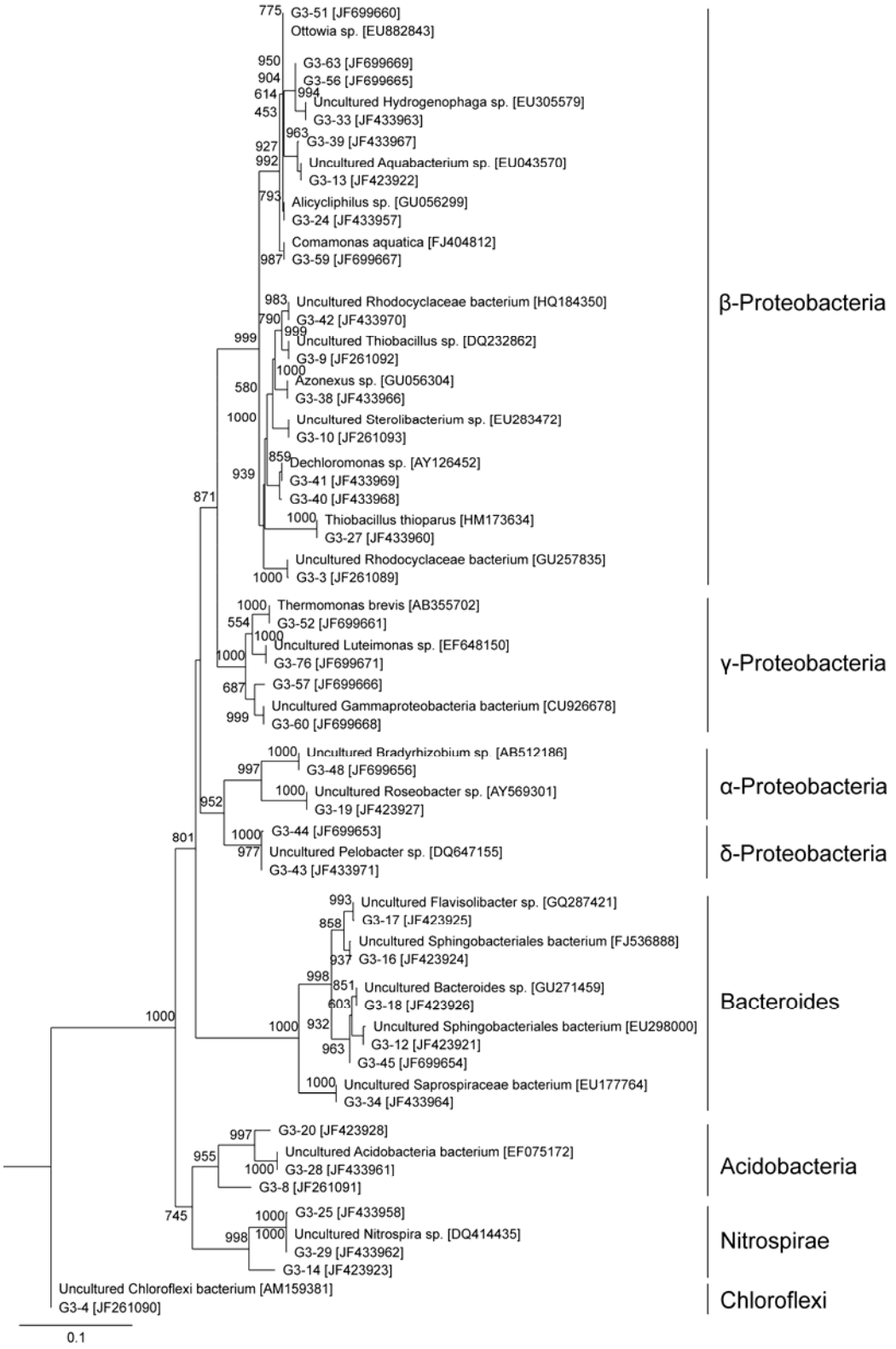

Figure 3.8: Maximum likelihood tree showing the phylogenetic relationship of bacteria based on partial sequence of 16S rDNA derived from aeration tank in STP 1. Bootstrap values (1000 replicates) of > 50% are shown on each branch. The scale bar represents 0.1 substitutions per base position.

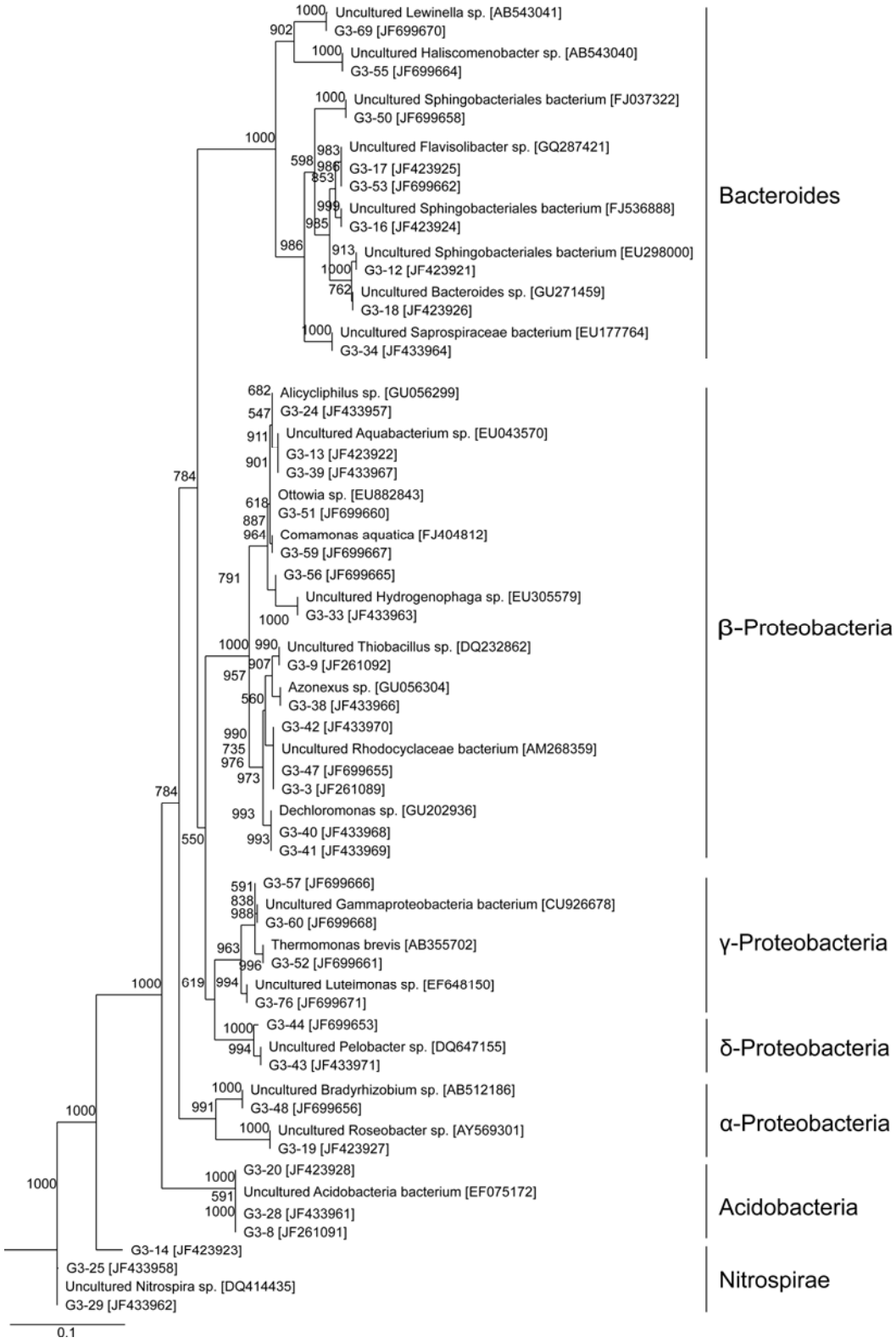

Figure 3.9: Maximum likelihood tree showing the phylogenetic relationship of bacteria based on partial sequence of 16S rDNA derived from aeration tank in STP 2. Bootstrap values (1000 replicates) of > 50% are shown on each branch. The scale bar represents 0.1 substitutions per base position.

Figure 3.10: Maximum likelihood tree showing the phylogenetic relationship of bacteria based on partial sequence of 16S rDNA derived from aeration tank in STP 3. Bootstrap values (1000 replicates) of > 50% are shown on each branch. The scale bar represents 0.1 substitutions per base position.

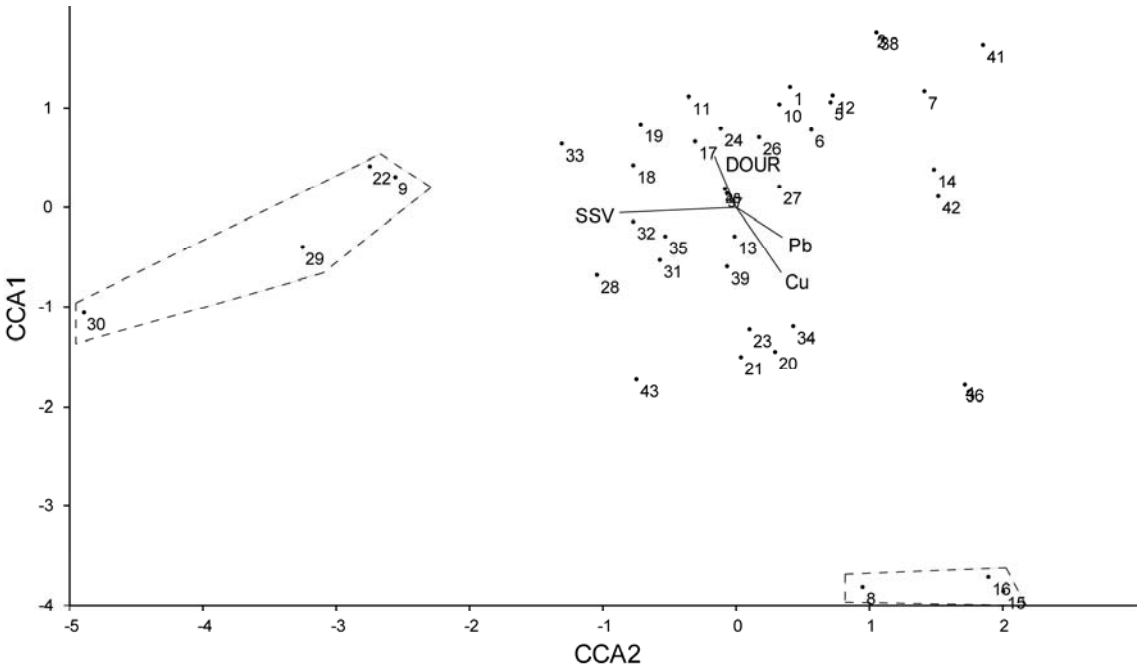

Figure 3.11: CCA showing the ecological distance of the bacterial community structure. The loading plots for DOUR, SSV, Pb and Cu are also shown. Two distinct groups are shown by the broken lines.